CASE STUDY OF 10TH ORDER ELLIPTIC AND QUASI-ELLIPTIC SELF-EQUALIZED MULTI-CAVITY FILTERS

J.W. Bandler and S.H. Chen

SOS-84-23-R

December 1984

CASE STUDY OF 10TH ORDER ELLIPTIC AND QUASI-ELLIPTIC SELF-EQUALIZED MULTI-CAVITY FILTERS

J.W. Bandler and S.H. Chen

Abstract

An interesting study of the development of 10th order multi-coupled cavity filters is presented. The dual-symmetrical coupling configuration is considered. Examples include a fully-elliptic filter with optimum amplitude and a quasi-elliptic self-equalized filter obtained from simultaneous optimization of group delay and amplitude. Both filters are synchronously tuned. Network variables as well as data related to the optimization process are provided.

This work was supported in part by the Natural Sciences and Engineering Research Council of Canada under Grant G1135.

The authors are with the Simulation Optimization Systems Research Laboratory and the Department of Electrical and Computer Engineering, McMaster University, Hamilton, Canada L8S 4L7.

I. INTRODUCTION

An approach to interactive design optimization of multi-coupled cavity microwave filters has been proposed in [1]. Implementing our approach on a CDC 170/730 digital computer, a computer program has been constructed and successfully tested for various filter design problems. An efficient method of filter simulation and sensitivity evaluation, namely the loaded filter approach, as presented in Section IV of [2], is utilized. Some selected numerical examples have been reported previously in [3].

Here, an interesting case study of the development of 10th order multi-coupled cavity filters is presented. Starting from an initial guess a primitive design is obtained using only amplitude specifications. Then by introducing phase and amplitude specifications simultaneously, a nonminimum-phase quasi-elliptic self-equalized design is generated which has superior group delay characteristics and is less sensitive to cavity dissipations. Based upon observation of the responses of the primitive design, the specifications are refined in order to overcome the stumbling-block of a local minimum and a fully elliptic filter with optimum amplitude is achieved by sequential optimization.

A review of the dual-symmetrical coupling pattern employed here can be found in Section III of [2]. In describing the filter responses, the following abbreviations are used: RC – reflection coefficient, RL – return loss, IL – insertion loss and GD – relative group delay.

II. THE FILTER MODEL

All the examples presented are based on a 10th order model, centered at 4000 MHz with 1% (40 MHz) bandwidth. The structure of the filter network is shown in Fig. 1. The nonzero elements of the coupling matrix **M**, as used for our examples, are illustrated in Fig. 2. The filter cavities are coupled in a dual-symmetrical pattern. This implies, in terms of the elements of **M**, that

$$M_{\ell k} = M_{k\ell} = M_{\sigma\tau} = M_{\tau\sigma}, \tag{1}$$

where $\sigma = n+1-\ell$ and $\tau = n+1-k$, n being the order of the filter.

The solutions of the examples are given in terms of the nonzero couplings and transformer ratios. Since the couplings are related by (1), only the distinct coupling values are given, e.g., for $M_{12} = M_{21} = M_{9,10} = M_{10,9}$, only M_{12} is given. The terminations, as shown in Fig. 1, are normalized such that we have the load resistor $R_L = 1\ \Omega$ and the voltage source $E = 1$ V with a resistor $R_S = 1\ \Omega$.

III. THE PRIMITIVE DESIGN

Solution

$$M_{12} = 0.81128$$

$$M_{23} = 0.58034$$

$$M_{34} = 0.52498$$

$$M_{45} = 0.52622$$

$$M_{56} = 0.56002$$

$$M_{1,10} = -0.00731$$

$$M_{29} = 0.04929$$

$$M_{38} = -0.17571$$

$$M_{47} = 0.09306$$

$$n_1^2 = n_2^2 = 0.96994$$

Simulated Responses

Lower stopband:		– 3976 MHz, minimum IL 61 dB
Passband:	3980 –	4020 MHz, minimum RL 20 dB
Upper stopband:	4024 –	MHz, minimum IL 61 dB

The simulated responses are also shown in Figures 3 and 4.

Starting Point

$$M_{12} = 0.8$$

$$M_{23} = 0.5$$

$$M_{34} = 0.55$$

$$M_{45} = 0.6$$

$$M_{56} = 0.5$$

$$M_{1,10} = 0.1$$

$$M_{38} = -0.1$$

$$M_{29} = -0.4$$

$$M_{47} = 0.4$$

$$n_1^2 = n_2^2 = 1.0$$

Table of Subinterval Data

Frequency edges of subinterval (MHz)	No. of sample points	Step-length of extrema location	Specification	Weighting factor
3950 – 3970	5	2.0	RC = 0.999995	–100.0
3970 – 3976	5	0.6	RC = 0.999995	–100.0
3980 – 3986	5	0.3	RC = 0.1	1.0
3986 – 4001	6	0.5	RC = 0.1	1.0

Optimization Parameters

Variables: $M_{12}, M_{23}, M_{34}, M_{45}, M_{56}, M_{1,10}, M_{29}, M_{38}, M_{47}, n_1^2$,

Initial step-length: 0.005

Accuracy requirement: 1.0×10^{-6}

Solution obtained after 150 iterations with 140 CPU sec.

Transfer Function Analysis

The voltage transfer ratio $H(s) \triangleq c\, N(s)/D(s)$, where

$$D(s) = \prod_{j=1}^{10} (s - p_j) \ , \quad N(s) = \prod_{i=1}^{8} (s - z_i) \quad \text{and} \quad c = j\,0.007094$$

The poles p_j: $-0.033692 \pm j\,1.028190$, $-0.121206 \pm j\,0.961854$, $-0.252062 \pm j\,0.776306$

$-0.342901 \pm j\,0.404486$, $-0.220079 \pm j0.081191$

The zeros z_i: $0.000000 \pm j\,1.836340$, $0.000000 \pm j\,1.341250$, $-0.000000 \pm j1.216028$

$\pm\, 0.283128 + j\,0.000000$

The pole-zero pattern of H(s) is shown in Fig. 5.

Real frequency loss poles (MHz): 3963.4, 3973.3, 3975.8, 4024.4, 4026.9, 4036.9.

Reflection zeros (MHz): 3980.2, 3981.8, 3985.7, 3997.6, 4002.4, 4008.3, 4014.3, 4018.2, 4019.9.

IV. A QUASI-ELLIPTIC SELF-EQUALIZED FILTER

Filter Type

Nonminimum-phase, quasi-elliptic self-equalized filter obtained from simultaneous optimization of group delay and amplitude.

Solution

$$M_{12} = 0.84424$$

$$M_{23} = 0.59318$$

$$M_{34} = 0.54438$$

$$M_{45} = 0.53059$$

$$M_{56} = 0.46916$$

$$M_{1,10} = 0.01597$$

$$M_{29} = -0.02673$$

$$M_{38} = -0.05570$$

$$M_{47} = 0.13067$$

$$n_1^2 = n_2^2 = 1.04566$$

Simulated Responses

Lower stopband:		–	3976	MHz, minimum IL 45.6 dB
Passband:	3980	–	4020	MHz, minimum RL 22 dB
Upper stopband:	4024	–		MHz, minimum IL 45.6 dB
Group delay:	3985	–	4015	MHz, maximum variation 4 ns
	3991	–	4009	MHz, maximum variation 1.5 ns

The simulated responses are also shown in Figures 6 and 7.

Starting Point

The solution of the primitive design.

Table of Subinterval Data

Frequency edges of subinterval (MHz)	No. of sample points	Step-length of extrema location	Specification	Weighting factor
3950 – 3968	4	fixed points	RC = 0.999995	–1000.0
3969 – 3976	4	1.0	RC = 0.999995	–1000.0
3980 – 3984	4	0.5	RC = 0.08	50.0
3984 – 4000	6	1.0	RC = 0.08	50.0
3985 – 4000	4	fixed points	GD = 1.5	1.0

Comment

The optimization of group delay is formulated using equations (10), (11) and (13) of [1], where the relative responses are defined as the magnitude of the difference between the average group delay and the group delay at the sample points.

Optimization Parameters

Variables: $M_{12}, M_{23}, M_{34}, M_{45}, M_{56}, M_{1,10}, M_{29}, M_{38}, M_{47}, n_1^2$

Initial step-length: 0.005

Accuracy requirement: 1.0×10^{-6}

Solution obtained after 24 iterations with 17.7 CPU sec.

Transfer Function Analysis

The voltage transfer ratio $H(s) \triangleq c\, N(s)/D(s)$, where

$$D(s) = \prod_{j=1}^{10} (s - p_j) \ , \ N(s) = \prod_{i=1}^{8} (s - z_i) \text{ and } c = j\,0.0166951$$

The poles p_j: $-0.044646 \pm j\,1.040871$, $-0.160270 \pm j\,0.954745$, $-0.274477 \pm j\,0.712155$

$-0.278207 \pm j\,0.414431$, $-0.288059 \pm j\,0.149511$

The zeros z_i: $0.000000 \pm j\,1.459862$, $0.000000 \pm j\,1.2222694$, $\pm\, 0.523371 \pm j\,0.328333$

The pole-zero pattern of H(s) is shown in Fig. 8.

Real frequency loss poles (MHz): 3970.9, 3975.6, 4024.5, 4029.3.

Reflection zeros (MHz): 3980.2, 3982.2, 3986.4, 3991.7, 3997.2, 4002.8, 4008.3, 4013.7, 4017.8, 4019.9.

Comment

Among the eight zeros of the transfer function, four are realized in real frequency as the attenuation poles and the other four form a complex quad in the s-plane. Such a nonminimum-phase design shows superior delay and amplitude characteristics. It is proved

that the sensitivity of the gain response w.r.t. dissipations is proportional to the group delay (see, for example, [4]). Hence a filter design with flat delay is also less sensitive to the cavity dissipations. Fig. 9 shows the insertion loss of our design with Q = 10,000. The loss variation is less than 0.1 dB over 80% of the passband.

V. A FULLY-ELLIPTIC FUNCTION FILTER

Comment

Elliptic function filters are known to have optimum amplitude characteristics in both the passband and the stopband. For these filters, all possible transmission zeros are realized in real frequency. But for the primitive design obtained previously, only six attenuation poles have presented themselves as shown in Fig. 3. We find, by inspection of the transfer function, that the missing pair of zeros are somehow located undesirably. Restart of optimization without any modification of the specifications has been attempted but failed to give a better solution. It turns out that the primitive design is a trapping local minimum. This is not too surprising since the starting point was almost arbitrarily chosen.

At this stage, some knowledge of the physical property of nonminimum- phase networks is quite helpful. As can be seen in Fig. 4, a group delay ripple is quite noticeable. Unmistakably, this ripple is the effect of the misplaced zeros. It is reasonable to believe that if we can suppress the group delay ripple by imposing an appropriate delay specification, a more desirable pole-zero pattern may result. The following data contains the refined specifications and the corresponding optimization results.

Starting Point

The solution of the primitive design.

Table of Subinterval Data

Frequency edges of subinterval (MHz)	No. of sample points	Step-length of extrema location	Specification	Weighting factor
3950 – 3970	5	2.0	RC = 0.999995	– 100.0
3970 – 3976	5	0.6	RC = 0.999995	– 100.0
3980 – 3981.5	3	0.3	RC = 0.05	1.0
3981.5 – 4000	7	0.5	RC = 0.05	1.0
3994, 4000*	2	fixed points	GD = 2.0	0.01

* Only two points near the center frequency are taken for group delay, since we are not optimizing the group delay over the passband but trying to suppress the ripple.

Optimization Parameters

Variables: $M_{12}, M_{23}, M_{34}, M_{45}, M_{56}, M_{1,10}, M_{29}, M_{38}, M_{47}, n_1^2$

Initial step-length: 0.01

Accuracy requirement: 1.0×10^{-5}

Solution obtained after 37 iterations with 30 CPU sec.

Solution

$$M_{12} = 0.91078$$

$$M_{23} = 0.61214$$

$$M_{34} = 0.55449$$

$$M_{45} = 0.51756$$

$$M_{56} = 0.67820$$

$$M_{1,10} = -0.00306$$

$$M_{29} = 0.02713$$

$$M_{38} = -0.08288$$

$$M_{47} = -0.09156$$

$$n_1^2 = n_2^2 = 1.2015$$

Simulated Responses

Lower stopband:		–	3976	MHz, minimum IL 54 dB
Passband:	3980	–	4020	MHz, minimum RL 26 dB
Upper stopband:	4024	–		MHz, minimum IL 54 dB
Group Delay:	3994	–	4000	MHz, maximum variation 4 ns

Comment

The group delay ripple has been suppressed as expected. The simulation shows a smooth delay response in the vicinity of center frequency. Taking this result as a starting point, we now release the delay specification and tighten the amplitude specifications, hoping that the next iteration will lead to an optimum amplitude design.

Table of Subinterval Data

Frequency edges of subinterval (MHz)	No. of sample points	Step-length of extrema location	Specification	Weighting factor
3930 – 3954	4	fixed points	RC = 0.99999995	– 1000.0
3959 – 3970	3	1.0	RC = 0.99999995	– 1000.0
3970 – 3976	4	0.4	RC = 0.99999995	-1000.0
3980 – 3981.5	3	0.3	RC = 0.032	1.0
3981.5 – 4000	7	0.5	RC = 0.032	1.0

Optimization Parameters

Variables: $M_{12}, M_{23}, M_{34}, M_{45}, M_{56}, M_{1,10}, M_{29}, M_{38}, M_{47}, n_1^2$

Initial step-length: 0.01

Accuracy requirement: 1.0×10^{-5}

Solution obtained after 190 iterations with 192 CPU sec.

Solution

$$M_{12} = 0.97284$$

$$M_{23} = 0.63006$$

$$M_{34} = 0.54981$$

$$M_{45} = 0.39867$$

$$M_{56} = 0.88914$$

$$M_{1,10} = 0.00298$$

$$M_{29} = -0.02422$$

$$M_{38} = 0.15196$$

$$M_{47} = -0.49440$$

$$n_1^2 = n_2^2 = 1.3415$$

Simulated Responses

Lower stopband: – 3976 MHz, minimum IL 70 dB

Passband: 3980 – 4020 MHz, minimum RL 30 dB

Upper stopband: 4024 – MHz, minimum IL 70 dB

The simulated responses are also shown in Figures 10 and 11.

Transfer Function Analysis

The voltage transfer ratio $H(s) \triangleq c\, N(s)/D(s)$, where

$$D(s) = \prod_{j=1}^{10} (s - p_j) \;, \quad N(s) = \prod_{i=1}^{8} (s - z_i) \quad \text{and} \quad c = j\,0.003996$$

The poles p_j: $-0.031290 \pm j1.041456$, $-0.109003 \pm j1.003058$, $-0.231187 \pm j0.899743$

$-0.406584 \pm j0.671067$, $-0.563434 \pm j0.258380$.

The zeros z_i: $0.000000 \pm j2.247661$, $0.000000 \pm j1.514408$, $0.000000 \pm j1.287780$ $0.000000 \pm j1.211824$.

The pole-zero pattern of H(s) is also shown in Fig. 12.

Real frequency loss poles (MHz): 3955.3, 3969.8, 3974.3, 3975.8, 4024.3, 4025.8, 4030.4, 4045.2

Reflection zeros (MHz): 3980.1, 3981.3, 3984.0, 3988.8, 3995.9, 4004.1, 4011.2, 4026.1, 4018.8, 4019.9.

VI. CONCLUSION

The practical application of optimization techniques is sometimes obstructed by the difficulty of local minima, especially when problems of large sizes and high nonlinearity are to be handled and/or the starting points are poorly chosen. Although a general solution is not available, in a particular case the difficulty can often be overcome by a combination of an adequate understanding of the problem with the CAD techniques. We have provided an illustration via the design of a high order elliptic function filter. We have also presented a nonminimum-phase example by which optimal tradeoffs between amplitude and group delay responses have been achieved. From these examples the flexibility and convenience in the treatment of various engineering specifications using modern CAD techniques can be better appreciated.

ACKNOWLEDGEMENT

The authors wish to thank S. Daijavad for the benefit of many discussions and suggestions.

REFERENCES

[1] J.W. Bandler and S.H. Chen, "Interactive optimization of multi-coupled cavity microwave filters", Department of Electrical and Computer Engineering, McMaster University, Hamilton, Canada, Report SOS-84-13-R, 1984.

[2] J.W. Bandler, S.H. Chen and S. Daijavad, "Efficient approaches to the simulation of narrow-band cavity filters", Department of Electrical and Computer Engineering, McMaster University, Hamilton, Canada, Report SOS-84-9-R, 1984.

[3] J.W. Bandler and S.H. Chen, "Selected numerical examples of design optimization of multi-coupled cavity microwave filters", Department of Electrical and Computer Engineering, McMaster University, Hamilton, Canada, Report SOS-84-15-R, 1984.

[4] J.W. Bandler, S.H. Chen and S. Daijavad, "Novel approach to multicoupled- cavity filter sensitivity and group delay computation", Electronics Letters, vol. 20, 1984, pp. 580-581.

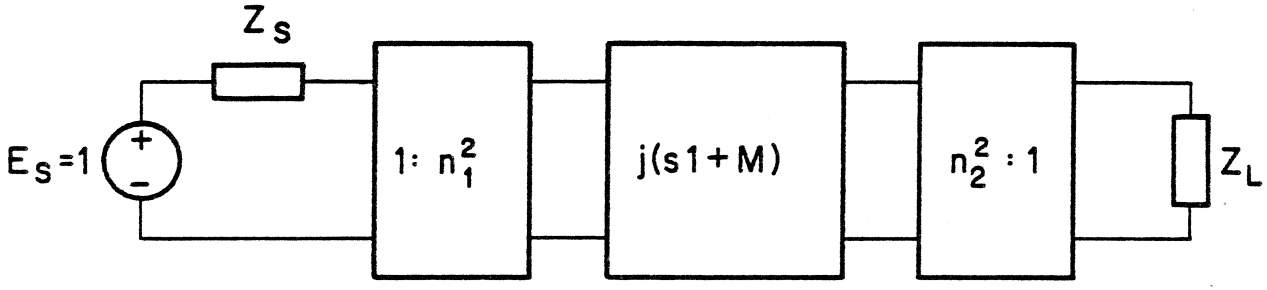

Fig. 1 Block representation of the overall network.

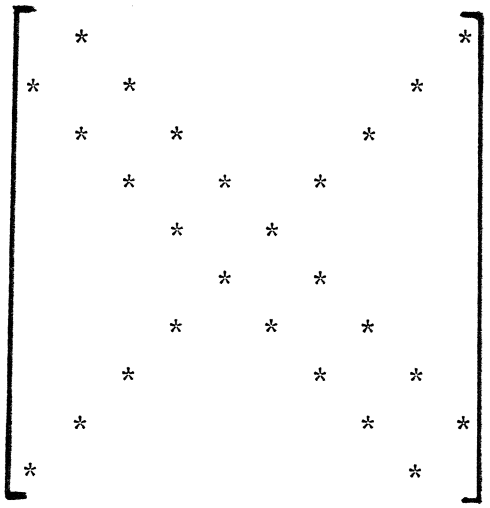

Fig. 2 Nonzero elements of the coupling matrix.

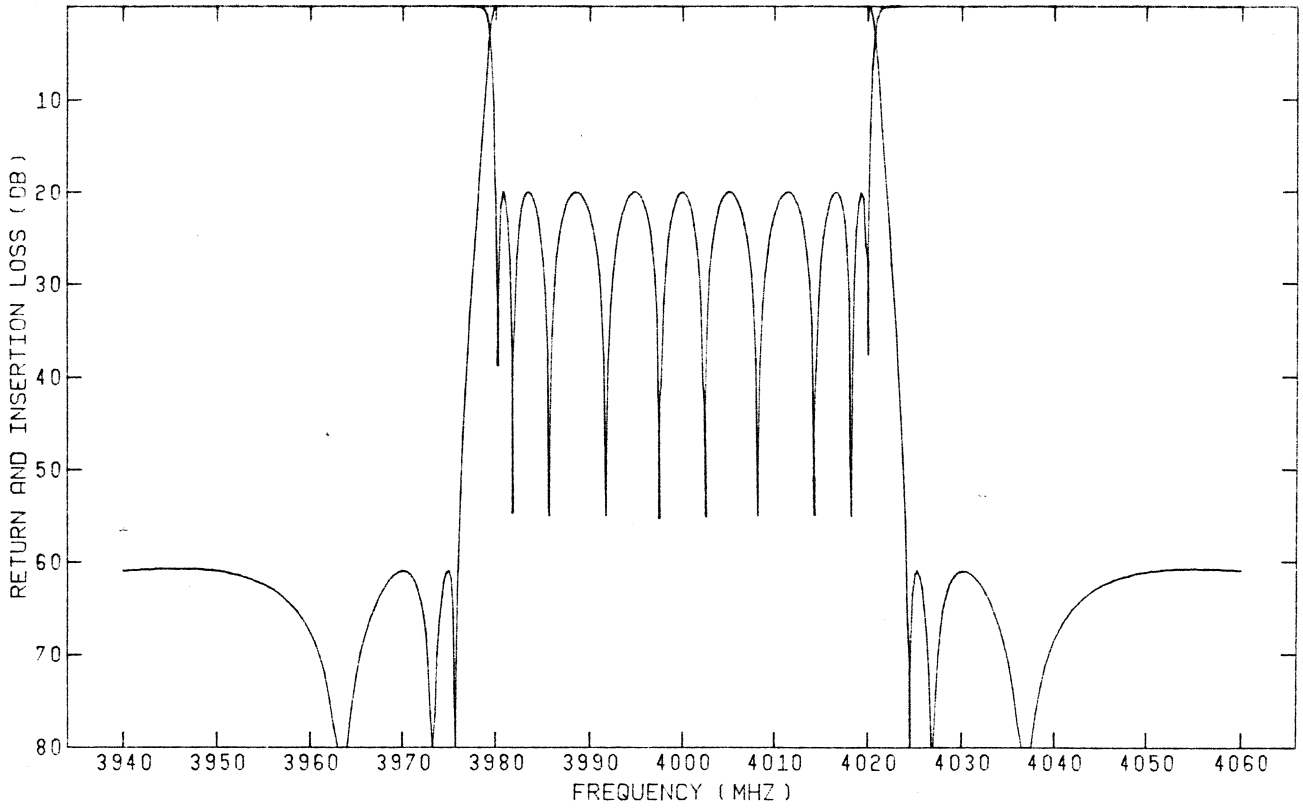

Fig. 3 Return and insertion loss of the primitive design.

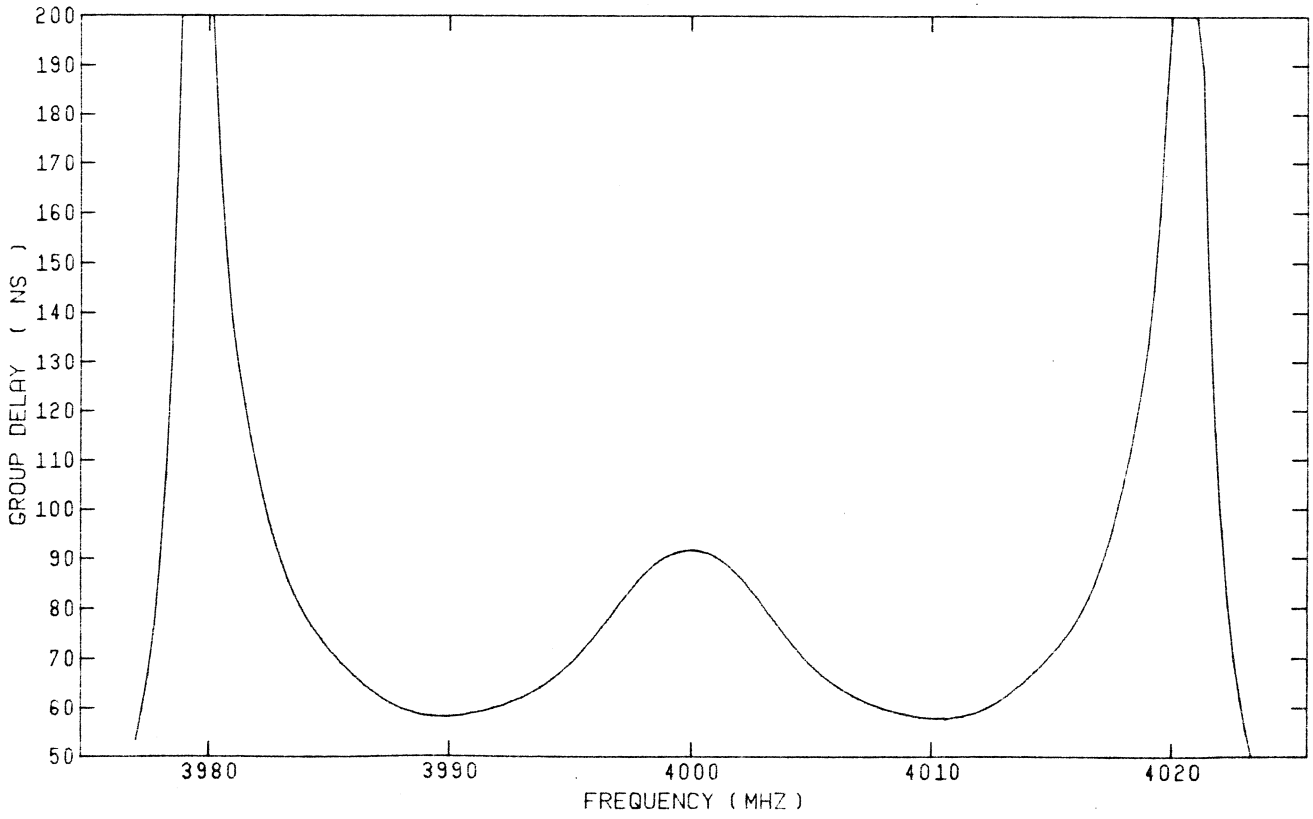

Fig. 4 Group delay response of the primitive design.

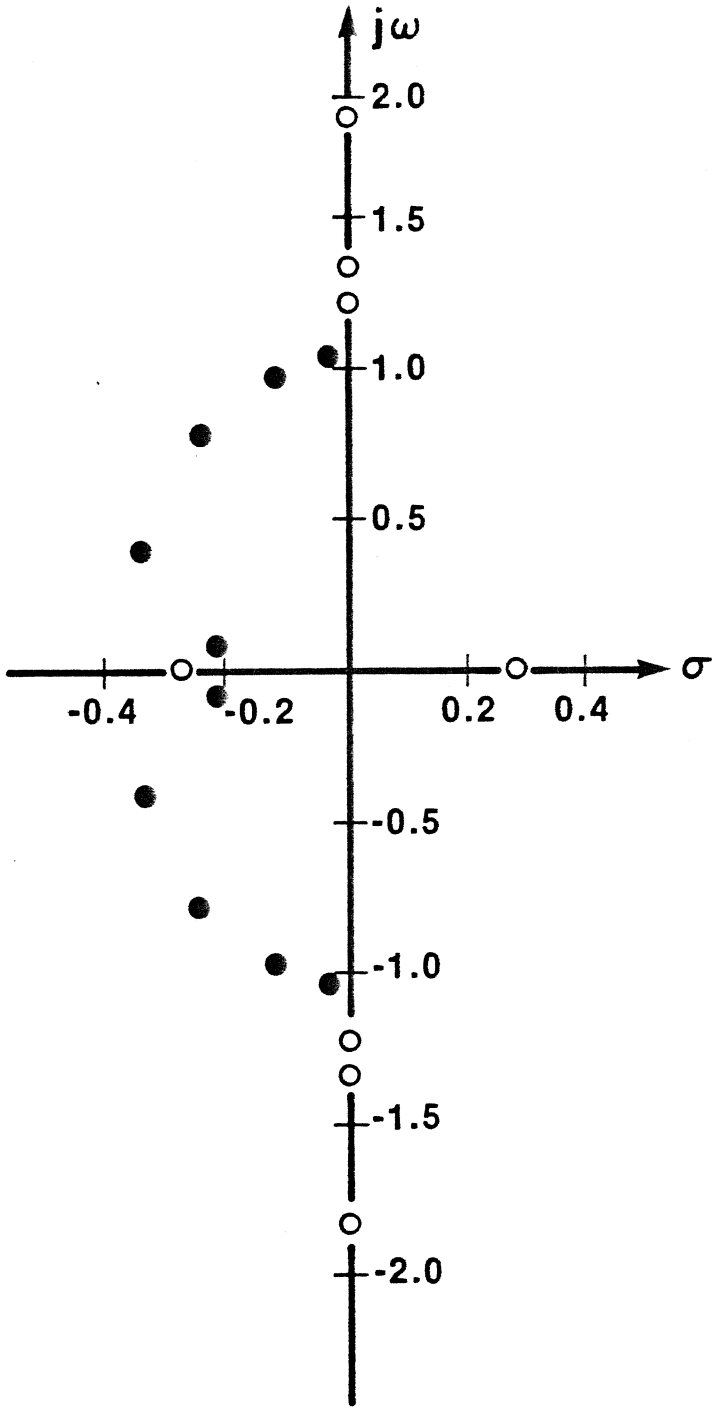

Fig. 5 Pole-zero pattern of the primitive design
●- poles , o - zeros

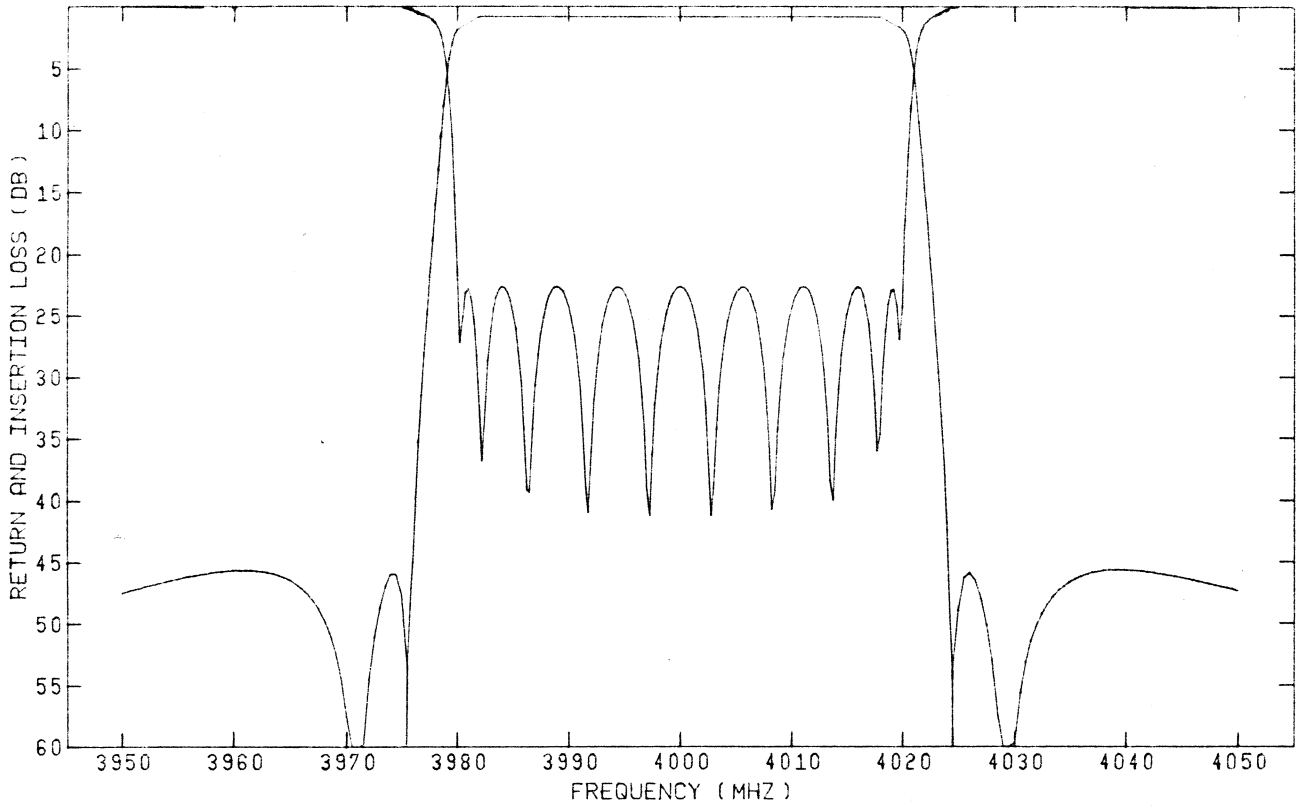

Fig. 6 Return and insertion loss of the quasi-elliptic self-equalized example.

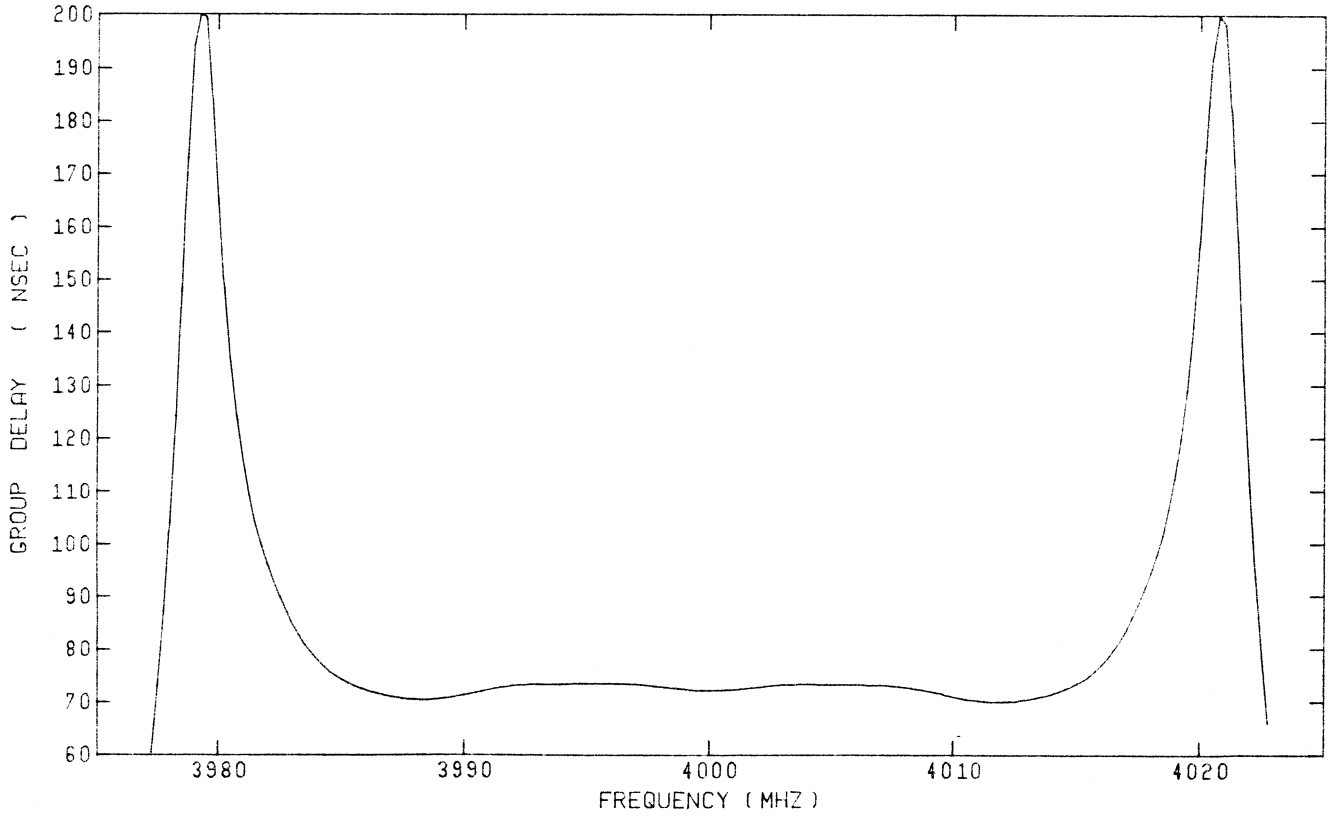

Fig. 7 Group delay response of the quasi-elliptic self-equalized example.

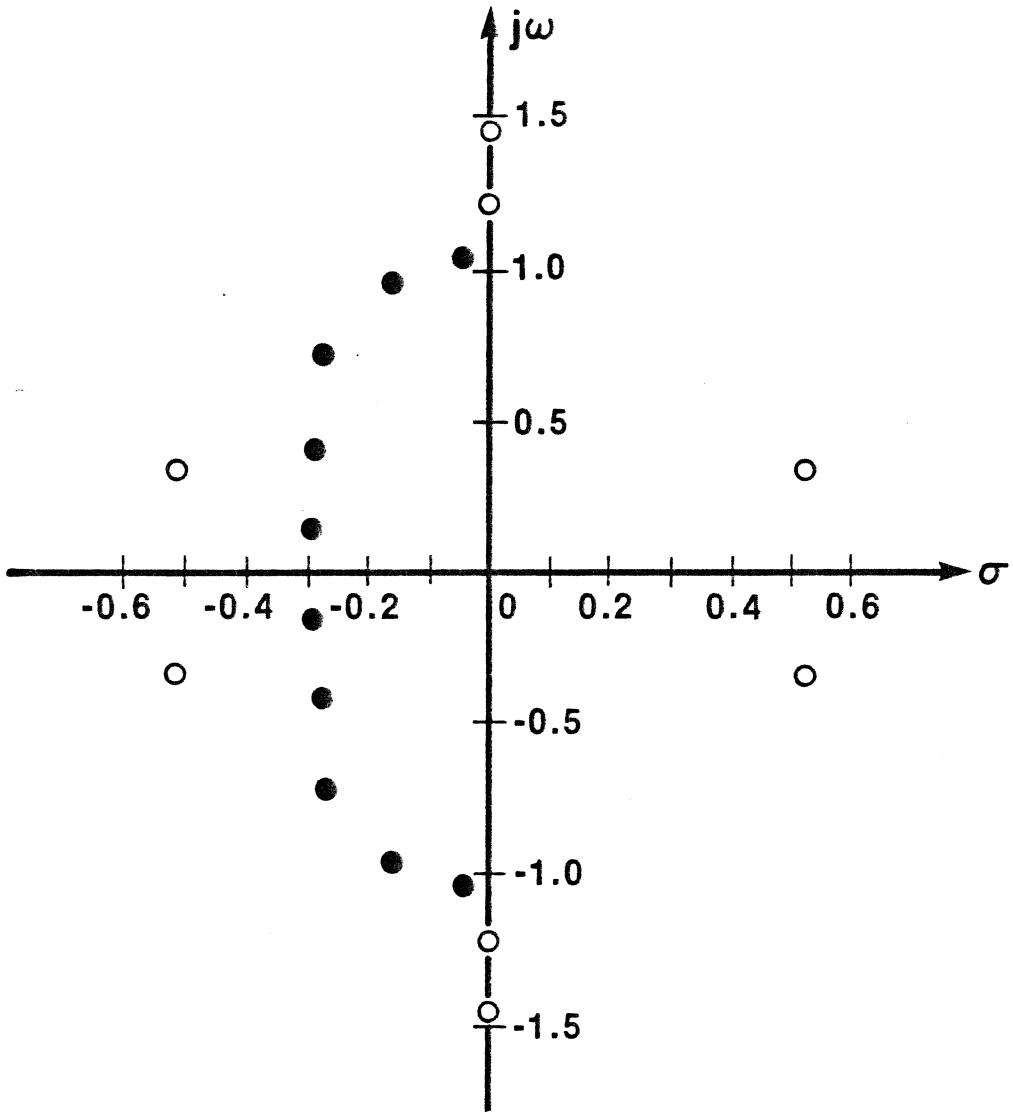

Fig. 8 Pole-zero pattern of the quasi-elliptic self-equalized example.
● - poles , o - zeros

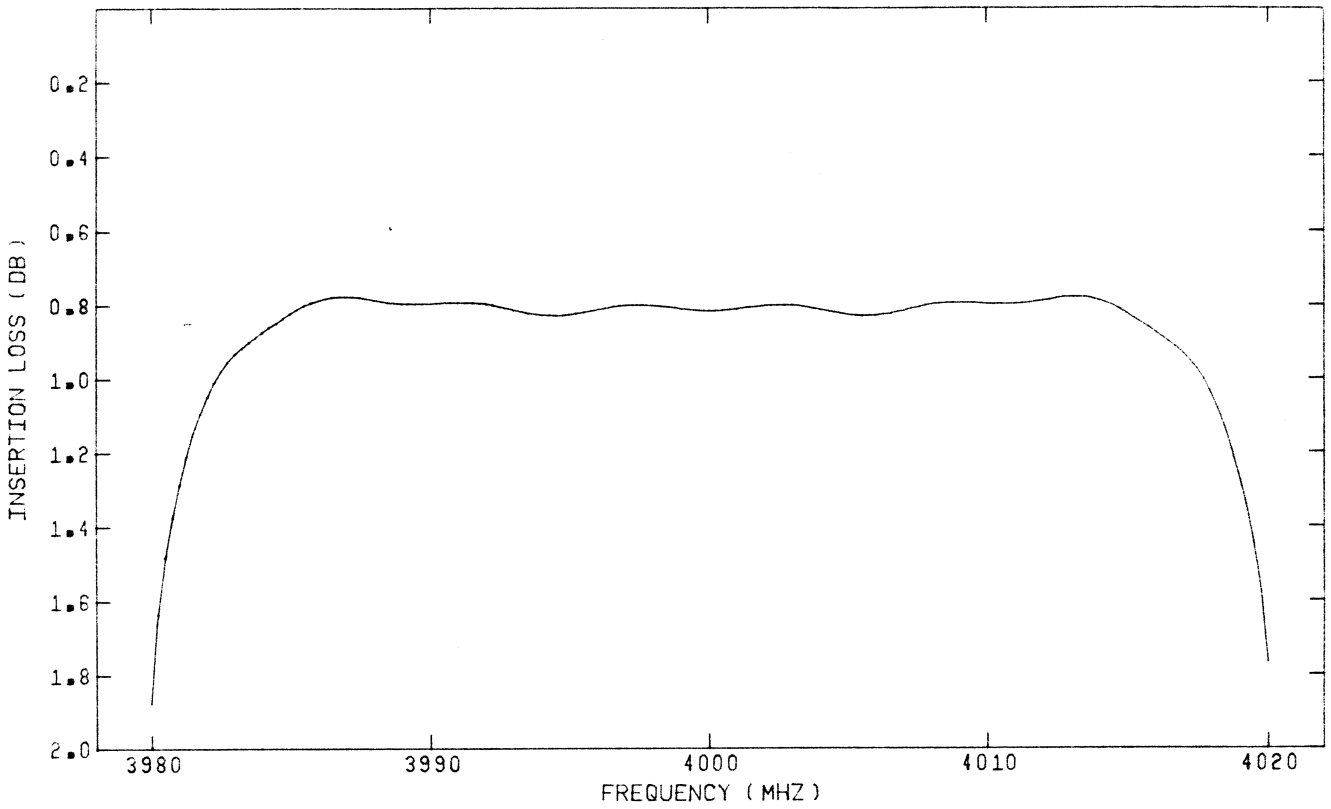

Fig. 9 Passband insertion loss of the quasi-elliptic self-equalized example with Q = 10,000

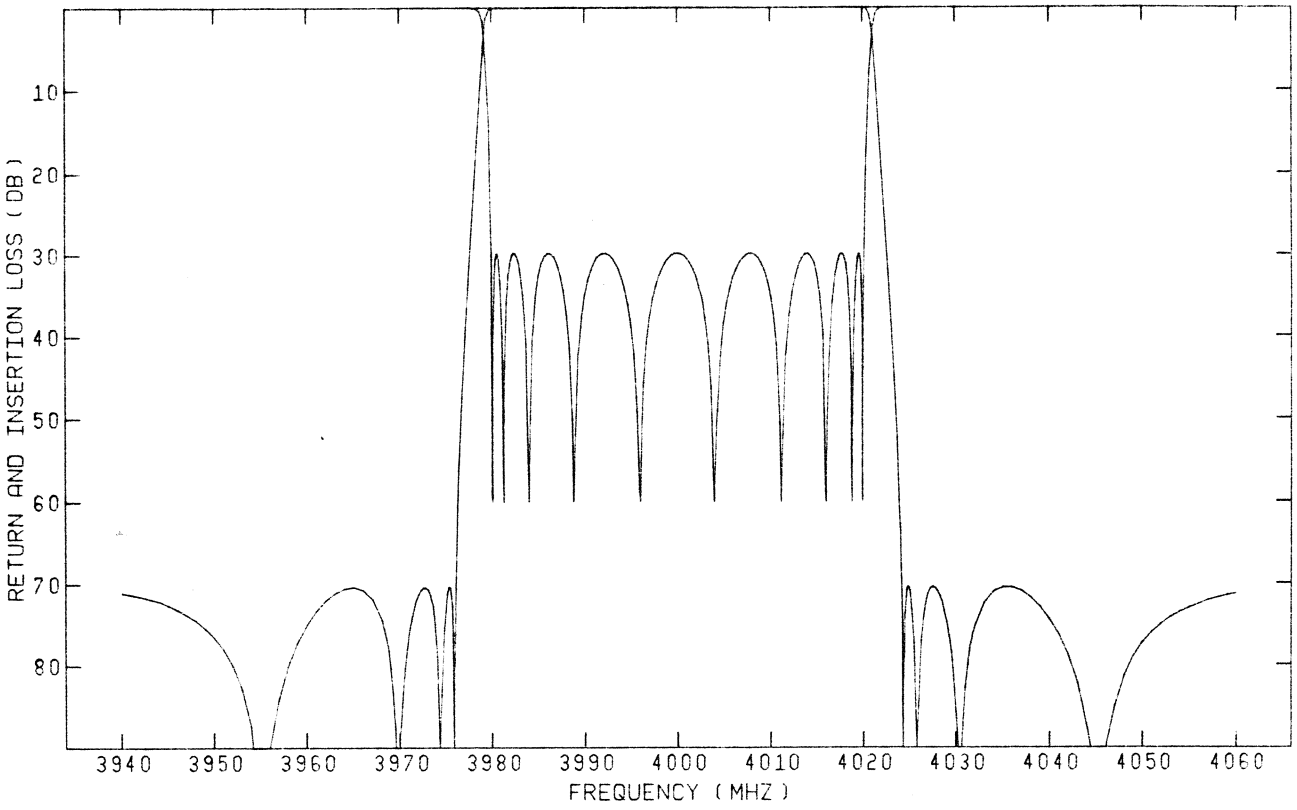

Fig. 10 Return and insertion loss of the fully-elliptic filter.

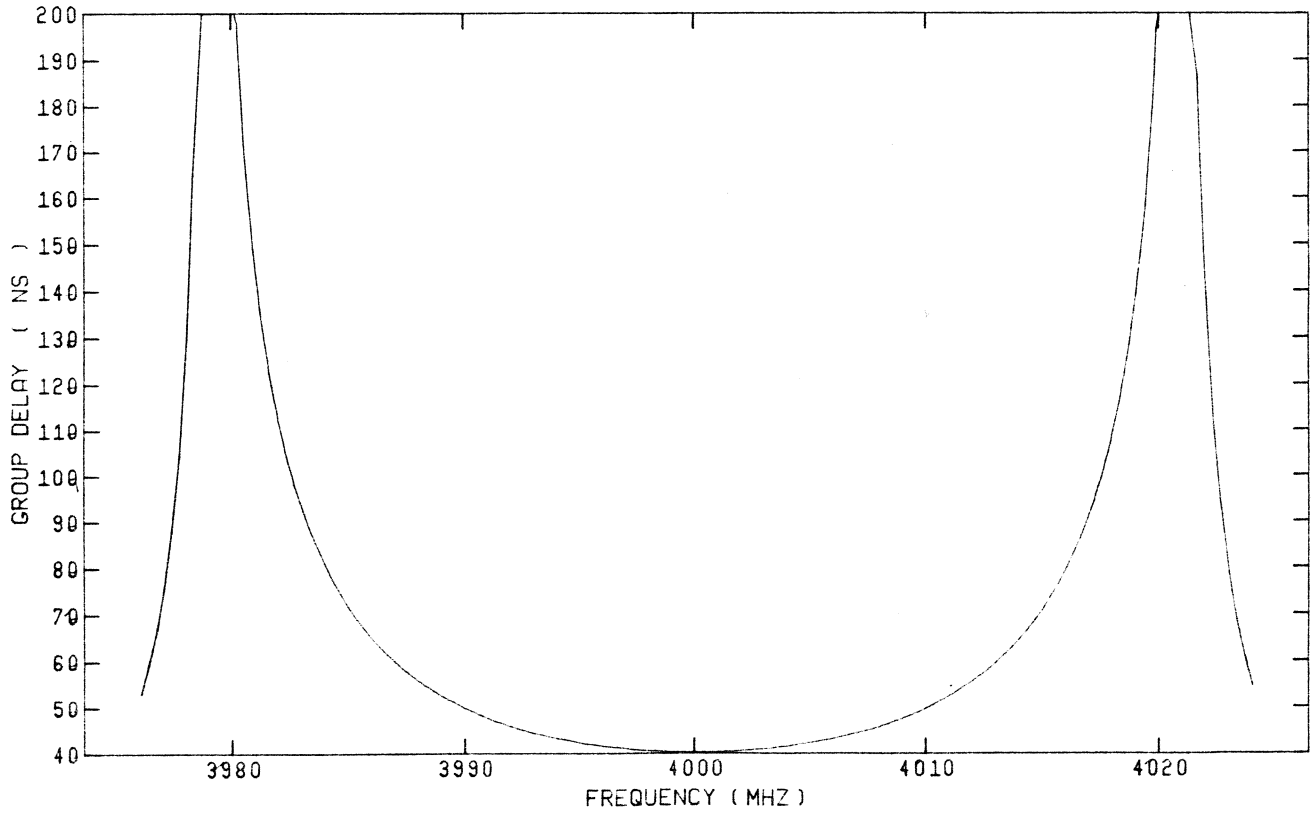

Fig. 11 Group delay response of the fully-elliptic filter.

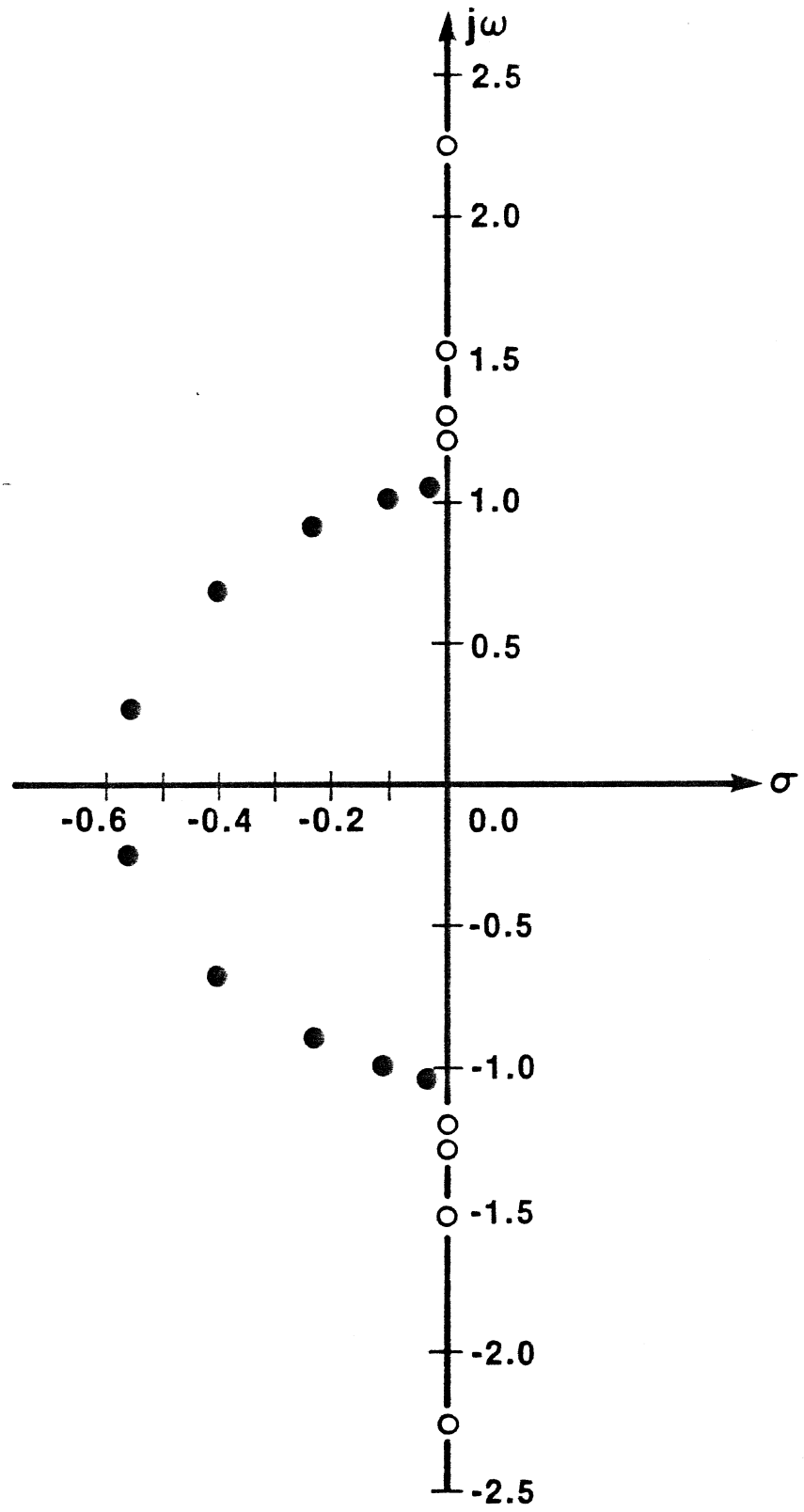

Fig. 12 Pole-zero pattern of the fully-elliptic filter
● - poles , o - zeros